SMST™ 2024: Extended Abstracts from the International Conference on
Shape Memory and Superelastic Technologies
May 6–10, 2024 , Cascais, Portugal
https://doi.org/10.31399/asm.cp.smst2024p0131

Ingot to Stent Part I – Microstructural and Corrosion Evaluation of Modern Nitinol Grades

Matthias Frotscher and Martin Kiekbusch
Cortronik GmbH, Rostock-Warnemünde, Deutschland

Stefan Riedl and Sebastian Knobloch
Vascotube GmbH (a Cirtec Company), Birkenfeld, Duetschland

Chad Thacker
Cirtec Medical, Brooklyn Park, MN, USA

Kyle Fezi and Jeremy E. Schaffer
Fort Wayne Metals Research Products, LLC, Fort Wayne, IN, USA Corresponding author jeremy_schaffer@fwmetals.com

Introduction

For producers and end-users of high-performance Nitinol, a material that functionally depends on everything that is done to it, it is critical to keep pace documenting the connection between producer-evolved grades and critical subcomponent performance. In Nitinol, the latitude of the industrial standard material specification ASTM F2063 should be continuously plied, and performance outcomes weighed against end-use demands as an aid to relevant use recommendations and requirements development [1]. The current standard specification for wrought NiTi requires maximum oxygen and carbon levels of 400 ppm and maximum observed contiguous particle- void-assembly (PVA) lengths not exceeding 39.0 microns measured in longitudinally mounted specimens. Performance variation across impurity- and PVA length-compliant nitinol grades, especially with respect to structural fatigue, is well documented where each new study gives a snapshot in time that depends on initial chemistry and PVA distributions, processing history, test coupon geometry, fatigue test boundary conditions, and other factors [2-4]. This study is a small step toward keeping pace with the connection between nitinol grades and tubing performance.

Materials

Nickel-rich binary NiTi alloy with 50.7 to 50.9 at% nickel content and supplier-certified to ASTM F2063 chemistry and inclusion ratings was sourced from four producers as 25 mm hot-worked diameter bar and machined to tube form via gundrilling. The melt origins were vacuum induction melting (VIM), vacuum arc melting (VAM), vacuum arc remelting (VAR), plasma arc melting (PAM), or a specific combination of these modalities applied to industrial grade input elements as described later with designation by the melt mode acronyms. These tubes were similarly processed via iterative annealing and mandrel cold working (Vascotube GmbH, Birkenfeld, Germany) to a subcomponent dimension of about 3.5 mm OD x 0.165 mm wall thickness prior to laser cutting, heat treatment with expansion, and electropolishing (Cortronik GmbH, Rostock, Germany).

Methods

This study evaluates changes of NiTi material properties and performance as a function of the initial grade and processing route, starting from the initial ingot material via the hot- and cold-working steps of a rod and tube respectively to the tubular subcomponent and finally a vascular stent. Focus is placed on commercially available VIM, VAR and/or PAM melt grades inserted into a standard 3.5 x 0.165 mm tube production process. Surface conditions were varied from as machined to electropolished. By assessing the microstructural evolution (e.g., grain size, texture formation, inclusion size and distribution) and improvements of the mechanical properties (e.g., plateau stresses, permanent set, and structural fatigue behavior), the influence of different material qualities and processing parameters on the final device performance are evaluated. Secondary phase particle analysis was conducted based on the standard ASTM WK84104 that is under development [5]. This method is, in part, visually demonstrated in Figure 1.

Metallographic samples were prepared by embedding in two-component epoxy Struers EpoFix with subsequent grinding on 800-4000 grit SiC paper and polishing with Struers DP-spray P 1µm and Cloeren Technology diamond lubricant. Scanning electron microscope (SEM) imaging was conducted with an FEI Quanta 250 FEG ESEM with field emission cathode in element contrast (acceleration voltage 10 kV, working distance = 10 mm, spot size = 5.0, pressure = 50 Pa).

A minimum area of 16 mm² was scanned for each sample to detect regions of interest with subsequent quantitative analysis of 12 images per sample taken at 500x magnification (field-of-view 252 x 217 µm with 0.2463 µm/px). Maximum inclusion size, maximum area fraction and particle size distribution were determined by automated image analysis using Olympus Stream V2.3.2 software.

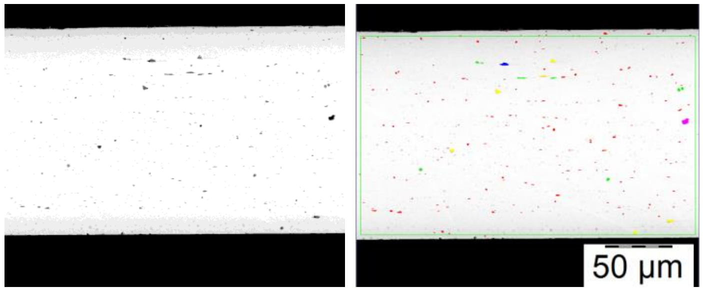

Figure 1: A region of interest field of view demonstrating SEM-based inclusion analysis of semi-finished nitinol stent tubing with BSE compositionally contrasted image (left) and threshold image (right). Image measurements, ROI: 34667 µm^2, Threshold: 200 (Value), Max Area Fraction/%: 0.579, Max Inclusion Size: 7.694 µm.

The microstructural changes were characterized by SEM, using the above-mentioned equipment and an EDAX TEAM Electron Backscatter Diffraction (EBSD) detector with DigiView V camera system. Apparent grain size was analyzed with Olympus Stream V2.3.2 software with the planimetry module based on ASTM E112 [6]. The texture evolution was observed by EBSD.

Electrochemistry was assessed by measuring 3 samples per material condition. Cyclovoltammetry was assessed per ASTM F2129 and galvanic corrosion potential was analyzed per ASTM F3044 using a 6-cell electrochemical setup with a BioLogic VMP3 Multichannel Potentiostat [7, 8].

The mechanical properties of the various material conditions (1-5) were analyzed by tensile testing using a Zwick Z20 electromechanical test system with temperature cabinet and a macroXtens extensometer testing at 37°C per ASTM F2516 [9].

Conclusions

This ongoing study is a multi-year installment that provides an updated and limited nitinol grade characterization for tube-based devices. The presentation of Part I will include: ingot transformation temperature data, particle-void assembly size distributions, and corrosion data.

References

[1] ASTM F2063-18 Standard Specification for Wrought Nickel-Titanium Shape Memory Alloys for Medical Devices and Surgical Implants, ASTM International, West Conshohocken, PA, 2021, DOI: 10.1520/F2063-18, www.astm.org
[2] Pelton, A. R., et al. "Fatigue and durability of Nitinol stents." Journal of the Mechanical Behavior of Biomedical Materials 1.2 (2008): 153-164.
[3] Toro, Alejandro, et al. "Characterization of non-metallic inclusions in superelastic NiTi tubes." Journal of Materials Engineering and Performance 18 (2009): 448-458.
[4] Robertson, Scott W., et al. "A statistical approach to understand the role of inclusions on the fatigue resistance of superelastic Nitinol wire and tubing." Journal of the Mechanical Behavior of Biomedical Materials 51 (2015): 119-131.
[5] ASTM WK84104 New Test Method for Determining the Particle and Inclusion size, and count in Nitinol products, under development in ASTM E04.14 on Quantitative Metallography, Technical Contact: Dr. Matthias Frotscher, ASTM International, West Conshohocken, PA, www.astm.org.
[6] ASTM E112-13(2021) Standard Test Methods for Determining Average Grain Size, ASTM International, West Conshohocken, PA, 2021, DOI: 10.1520/E0112-13R21, www.astm.org
[7] ASTM F2129-19a Standard Test Method for Conducting Cyclic Potentiodynamic Polarization Measurements to Determine the Corrosion Susceptibility of Small Implant Devices, ASTM International, West Conshohocken, PA, 2019, DOI: 10.1520/F2129-19A, www.astm.org.
[8] ASTM F3044-20 Standard Test Method for Evaluating the Potential for Galvanic Corrosion for Medical Implants, ASTM International, West Conshohocken, PA, 2020, DOI: 10.1520/F3044-20, www.astm.org.
[9] ASTM F2516-22 Standard Test Method for Tension Testing of Nickel-Titanium Superelastic Materials, ASTM International, West Conshohocken, PA, 2022, DOI: 10.1520/F2516-22, www.astm.org.